Computational Investigation of The Structures and Energies of Microporous Materials

Edward Stacey [a,b*], Matthew G. Quesne [a,b], C. Richard A. Catlow [a,b,c]

[a] School of Chemistry, Cardiff University, Main Building, Park Place, Cardiff CF10 3AT, UK

[b] UK Catalysis Hub, Research Complex at Harwell, STFC Rutherford Appleton Laboratory, Didcot, Oxfordshire OX11 0FA, UK

[c] Department of Chemistry, University College London, 20 Gordon St., London WC1 HOAJ, UK.

Abstract

We present a comprehensive study of calculated lattice and cohesive energies for pure silica zeolites and pure microporous alumino-phosphates (ALPOs). Molecular mechanical and quantum mechanical methodologies based on Density Functional Theory (DFT) are employed to calculate respectively lattice and cohesive energies, whose values relative to those of the dense α-Quartz (SiO_2) and Berlinite ($AlPO_4$) phases are compared to experimental values. The results confirm that the siliceous zeolites and microporous ALPOs are all metastable with respect to α-Quartz and Berlinite with the energy differences between the microporous and dense phases, calculated by the DFT methods for the siliceous systems being closer to experiment than those with the interatomic potential based methods; although calculations based on shell model potentials gave values closer to experimental values than those based on the rigid ion model and can reproduce the trends observed in both DFT and experiment at a low computational cost. For the zeolitic structures, interatomic potential based calculations tend to overestimate lattice energies which may arise from inadequacies in the modelling of charge transfer which can be modelled by the DFT studies. For the ALPO systems, DFT gives higher energies than the interatomic potential based methods which deviate appreciably from the experimental data. Possible origins of the discrepancy are discussed.

Keywords

Computational Chemistry; DFT; Interatomic potentials; Zeolites; ALPO

1. Introduction

It is well established that microporous materials are metastable with respect to dense polymorphs(Cundy & Cox, 2003; Navrotsky et al., 2009) and indeed useful correlations have been established between the energies of siliceous zeolites with respect to that of α-Quartz and framework density(Majda et al., 2008; Pophale et al., 2011). Computational methods have been used extensively to model structures and energetics of microporous frameworks, but the extent to which different computational techniques can predict quantitatively experimental thermodynamic data is not clearly established. This study provides a detailed assessment of both interatomic potential based lattice energy and DFT techniques in modelling framework energies of both siliceous zeolites and microporous ALPOs. We show that for the former, DFT techniques can achieve chemical accuracy when compared with experimental calorimetric data for siliceous zeolites. The agreement is less good for the ALPOs which we speculate may be attributable to greater differences between the models used and the systems investigated experimentally.

2. Methodology

As noted, we employ interatomic-potential based and quantum mechanical techniques. Lattice energy minimisations have previously been performed using a shell model on both silicates and alumino-phosphates with good agreement between experimental and calculated structures.(Henson et al., 1994)(Henson et al., 1996) In this study, lattice energy minimisation calculations utilise the General Utility Lattice Program (GULP)(Cope & Dove, 2007; Gale, 1997, 2005, 2006; Gale et al., 2011; Gale & Rohl, 2010, 2011), which required only modest computer resources and could be run locally, whereas the latter quantum mechanical method was run using Density Functional Theory (DFT) remotely on a high-performance computer.

Buckingham Potential	A (eV)	ρ (Å)	C (eV· Å^6)
Si^{4+}- O^{2-}	1283.9073	0.32052	10.66158
O^{2-} - O^{2-}	22764.3	0.149	27.88

Core – Shell Potential	k (eV·Å^{-2})
O^{2-}	74.92

Coulombic Charges	Si^{4+}	O^{2-}core	O^{2-}shell
	+4	+0.86902	-2.86902

Three-Body Term		Si core O shell O shell		
K (eV rad^{-2})	θ_0			
2.09724	109.47	1.8	1.8	3.2

Potentials as derived for silica structures by Sanders et al(Sanders et al., 1984)

Table 1. Zeolite Core-Shell Interatomic Potentials

2.1. Classical Lattice Energy Calculations

The GULP program sums electrostatic interactions and short-range potentials between different atomic species and has proved to be a valuable and effective tool for modelling microporous systems (Dorta-Urra & Gulín-González, 2006; González et al., 1999; Stojakovic & Rajic, 2001). Most of the current study employs the shell model (Dick & Overhauser, 1958) approach, whereby silicon, aluminium and phosphorus atoms act as single formal point-charges interacting via a specified forcefield, whilst the oxygen atoms comprise a core and a shell component, where the forces acting on the shell cause displacements which models the formation of a dipole. Additional calculations were performed with rigid ion potentials in which the O atom is also treated as a single point charge. The short-range potentials employed are of the Buckingham form(Buckingham et al., 1938):

$$\Phi_{12}(r) = Aexp\left(\frac{-r}{\rho}\right) - \frac{C}{r^6}$$

Where A, rho (ρ) and C are constants.. With the shell model the silicate systems used parameters derived by Sanders *et al*(Sanders et al., 1984) given in **Table 1**, and the potentials utilised for the ALPO structures were derived by Gale *et al*(Gale & Henson, 1994) given in **Table 2**, both employ a cut-off of 12Å. For the siliceous systems, a three-body term is employed via a quadratic energy term, defined as $E_B=\frac{1}{2} K_B(\theta-\theta_0)^2$ whereby $(\theta-\theta_0)$ is the deviation from the idealised tetrahedral angle for O-Si-O of 109.47° and K_B is a harmonic force constant for the bond bending component of the potential so that a representation of the directionality of the Si-O bonding is included.

Buckingham Potential	*A* (eV)		*ρ* (Å)	*C* (eV·Å^6)
Al^{3+}- O^{2-}	1460.30		0.29912	0.00
P^{5+}- O^{2+}	877.34		0.35940	0.00
O^{2-} - O^{2-}	22764.3		0.149	27.88
Core – Shell Potential			k (eV·Å^{-2})	
O^{2-}			74.92	
Coulombic Charges	P^{5+}	Al^{3+}	O^{2-}_{core}	O^{2-}_{shell}
	+5	+3	+0.86902	-2.86902
Three-Body Term			Td core O shell O shell	
K (eV rad^{-2})	θ_0			
2.09724	109.47	1.8	1.8	3.2

Potentials for ALPO structures provided by Gale and Henson(Gale & Henson, 1994)

Table 2. ALPO Core-Shell Potentials

In the case of rigid ion calculations, a partial charge model was adopted, using the parameters derived by Van Beest *et al*(van Beest et al., 1990), given in **Table 3,** with a cut-off of 4Å was employed, close to that used in the original

parameterisation, as confirmed through benchmarking shown in **Table S1** (See supporting information) , and yields energies in closer agreement to the experimental data. We note that this model does not include bond-bending terms.

Buckingham Potential	A (eV)	ρ (Å)	C (eV·Å6)
$Si^{2.4+}$- $O^{1.2-}$	18003.7572	0.2052	133.5381
$O^{1.2-}$ - $O^{1.2-}$	1388.773	0.3623	175.0
Coulombic Charges	$Si^{2.4+}$core	$O^{-1.2}$core	
	+2.4	-1.2	
Three-Body Term		Si core O shell O shell	
K (eV rad^{-2})	θ_0		
2.09724	109.47	1.8	1.8 3.2

Potentials for Rigid Ion model derived by Beest et al(van Beest et al., 1990)

Table 3. Zeolite Partial Charge Rigid Ion Potential Parameters

The calculations using these parameters carried out full geometry optimisations of both cell dimensions and atomic coordinates. This predominantly results in a slight increase of around 2% of unit cell volume as the structure relaxes but can reach up to 10 % for certain structures like CIT-5. For those systems with larger deviations after optimisation, the experimental composition typically differs appreciably from the purely siliceous model used here.

To contextualise the results of these internal energy values, additional free energy minimisation calculations were also undertaken using the GULP code. This methodology calculated the bulk geometrical lattice properties under a constant pressure and at a temperature of 298K with calculation of the vibrational entropies of the system. However, the differences between the calculated absolute energies of the entire lattice and free energies were very small (<1% difference in normalised energy values) and the contribution to the key energy differences between microporous and dense structures can for purposes of this study be omitted.

All structures in both the potential-based and DFT modelling were taken using structural data files provided by the Structure Commission of the International Zeolite Association (IZA-SC).(Ch. Baerlocher and L.B. McCusker, n.d.) with the α-Quartz structure taken from the work of Ogata *et al*(Ogata et al., 1987), and Berlinite's structure taken from the work of Sowa *et al*(Sowa et al., 1990).

2.2. Density Functional Theory

The optimisation of pure silica zeolites and pure ALPO structures using DFT was carried out using the VASP code(Kresse & Furthmüller, 1996a, 1996b; Kresse & Hafner, 1993, 1994). Previous studies have assessed the ability of various PBE functionals to model neutral-framework zeotypes(Fischer & Angel, 2017). In this study we employed the Perdew Burke-Ernzerhoff (PBE)(Perdew et al., 1996) generalized-gradient-approximation (GGA) for valence electrons which were generated with conventional LDA reference configurations(Perdew & Zunger, 1981), whilst the core was treated with PAW potentials(Joubert et al., 1999). A large k-point mesh of 5x5x5 was applied to account for long-range order effects. A Gaussian smear, which is typically used for metals, ensured that more of the k-points were on the Fermi surface. The role of long-range dispersion forces, such as van der Waals, have proven to be highly important in modelling the trends in stability in porous materials(Román-Román & Zicovich-Wilson, 2015). With this in mind, the Grimme D3 dispersion correction(Grimme et al., 2010) was employed in our calculations, which has been shown to improve the modelling of microporous structures(Fischer et al., 2014). A 520 eV planewave cut-off was used as it gave a reliable convergence criterion, along with a force convergence of -0.01 and an SCF cut-off of -0.00001 eV.

3. Results and Discussion

Results of our modelling of siliceous zeolites are first presented followed by those for the microporous ALPOs. Lattice energies are normalized with respect to the number of tetrahedral units and reported in kJ.

3.1 Zeolites: Classical – Shell Model with Formal Charges

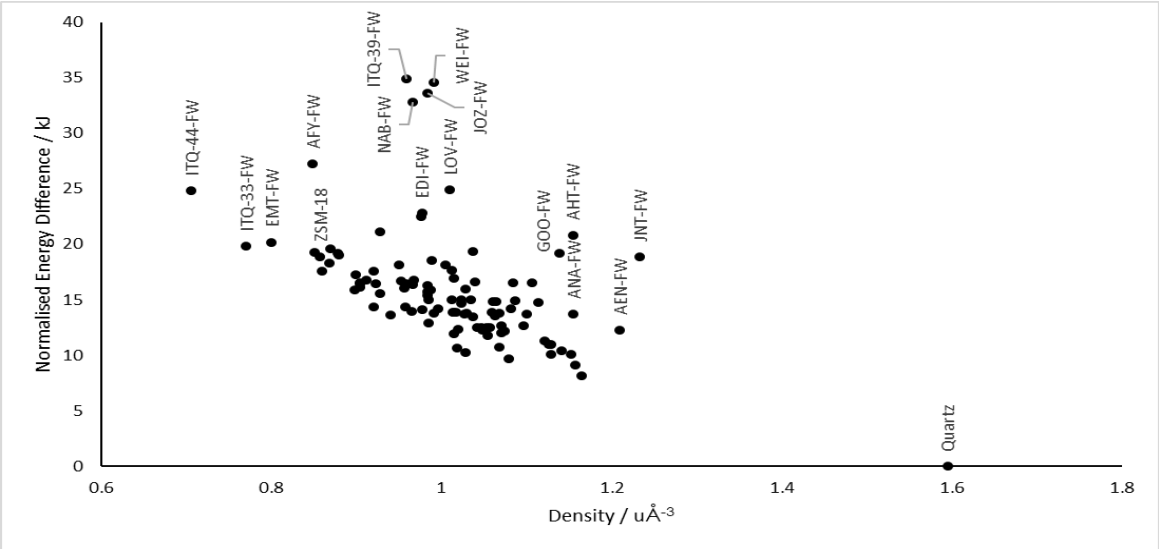

Fig. 1. Interatomic Potential Zeolite Lattice Energies Relative to α-Quartz

Figure 1 presents the calculated lattice energies per T atom with respect to that of α-Quartz, with values presented in **Table S2 (see supporting information)**: α-Quartz is used as a reference as it has the highest density and is the lowest energy tetrahedrally coordinated silica polymorph (when disregarding higher pressure phases) as a functional of density, defined as total atomic mass of the system divided by the volume of the unit cell.

As noted, Free-Energy Minimisation calculations were also performed at 298K to account for the entropic contributions on 13 structures with up to 24 T-sites to reduce the computational demand. The difference observed was less than 1% of the absolute lattice energies and so subsequently the entropic effects at ambient temperatures were deemed small enough to be considered negligible.

As expected, all structures are metastable with respect to quartz with a correlation for many with density, where most structures follow a roughly linear trend in terms of normalised energy, with some deviation. Indeed, substantial deviations from this trend are particularly apparent in the JOZ, WEI, EDI, LOV and NAB frameworks (FW). WEI is not technically an alumino silicate; since, when synthesised it forms a framework consisting of P, Be and Ca atoms which could account for this discrepancy. A similar caveat can be applied to the other structures, whilst they contain silicon there are significant contributions to the framework from other elements: JOZ contains Be within its framework, LOV's structure contains Na and Be and NAB contains both Be and Na in its framework whereas EDI contains Al and Ba. Other outliers such as AHT, AFY and JNT can be attributed to the fact they are only synthesised as ALPO structures and not alumino silicates. ITQ-39 is a partially disordered material (intergrowth) which could be a significant factor regarding its higher energy. It should also be noted that these results are in line with the earlier findings of Henson(Henson et al., 1994) *et al* who adopted the same methodology.

3.2 Zeolites: Classical – Rigid Ion with Partial Charges

The partial-charge, rigid-ion model was next utilised to determine the extent and effect that ionic charge contributed to the relative energies of microporous and dense phases. The Buckingham potentials used were derived by Van Beest *et al*(van Beest et al., 1990) and are given in **Table 3**. The resultant energy values are presented for a selection of systems in **Table 4**, which shows that generally the partial charge model tends to calculate somewhat higher lattice energies than the Sanders formal charge shell model. However, for 2 structures: BEA and EMT lower energies were calculated. The reason for this different behaviour is not clear, although we note that BEA is a partially disordered material which may be relevant.

Structure	Van Beest / kJ	Sanders / kJ	ΔB-S / kJ
AST	19.23	18.15	1.08
BEA	13.50	14.39	-0.89
CFI/CIT-5	16.65	12.65	4.00
CHA	17.74	16.14	1.60
IFR/ITQ-4	15.71	14.99	0.72
ISV/ITQ-7	17.92	16.44	1.48
ITE/ITQ-3	14.41	14.12	0.20
MEL/ZSM-11	13.02	10.76	2.26
MFI/ZSM-5	12.48	9.68	2.80
MWW/ITQ-1	17.39	14.37	3.02
STT/SSZ-23	16.53	14.70	1.83
AFI	16.76	11.93	4.83
EMT	19.02	20.14	-1.12
FER	13.68	11.78	1.90
MEI/ZSM-18	23.39	18.85	4.54
MTQ/ZSM-12	11.48	8.16	3.32

Where ΔB-S is the difference between Van Beest and Sanders normalised energies

Table 4. Van Beest vs Sanders Potentials: Energy Differences of Siliceous Zeolites with respect to α-Quartz, Normalised to the Number of Tetrahedral Sites in the Unit Cell

3.3 ALPOs: Classical Shell Model

Again, the shell model was employed for this study, whereby both aluminium and phosphorus cations act as a rigid ion core whilst the oxygen atoms have a core and a shell to model polarizability. The potentials were taken from Gale(Gale & Henson, 1994) *et al* and are reported in **Table 2**. This set of data was again normalised to each T-site and the energy difference calculated relative to that of Berlinite, the simplest dense polymorph, to which Gale's potentials were fitted; the results are reported in **Table S3** (see supporting information) and illustrated diagrammatically in **Figure 2**. As expected, we see a clear linear trend between energy and density of these structures with Berlinite as the densest, lowest energy polymorph.

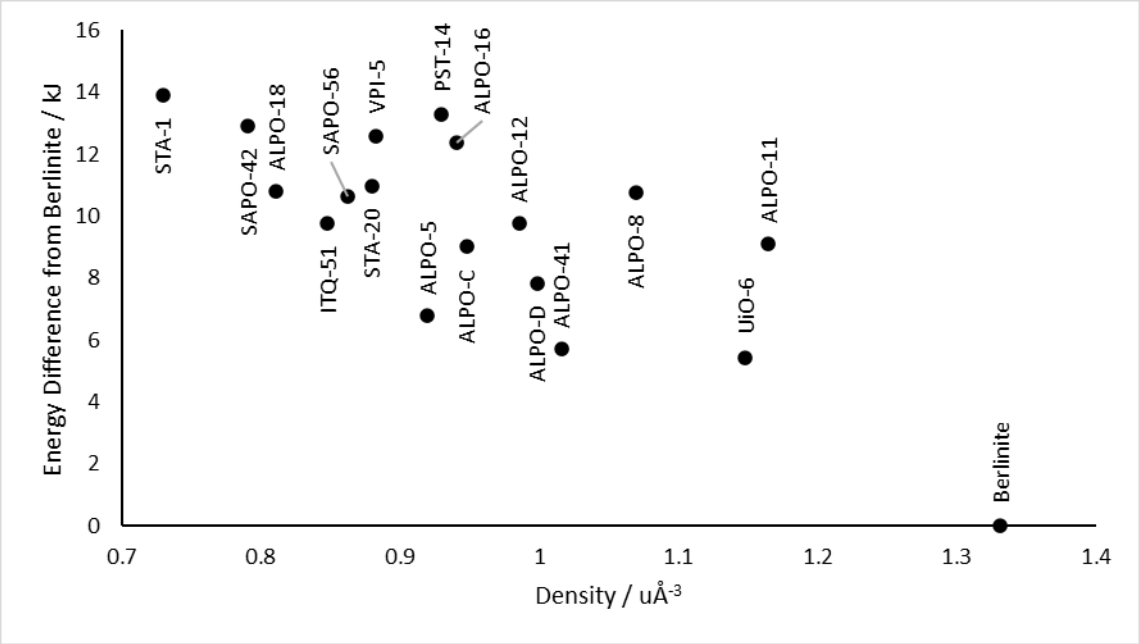

Fig. 2. Normalised Interatomic Potential ALPO Lattice Energies per T-site Relative to Berlinite vs Density

3.4 DFT: Zeolites

Results from the DFT calculations were again normalised to the number of T-sites as in the previous section, and the energy differences were calculated with respect to α-Quartz. The results are reported in **Table S4 (see supporting information)**. When plotting the difference in energy against the density, as shown in **Figure 3**, a linear trend is once again observed with a similar distribution to the lattice energy results in **Figure 1.** Once again, α-Quartz has the highest density, and the results re-affirm the relationship between density and cohesive energy.

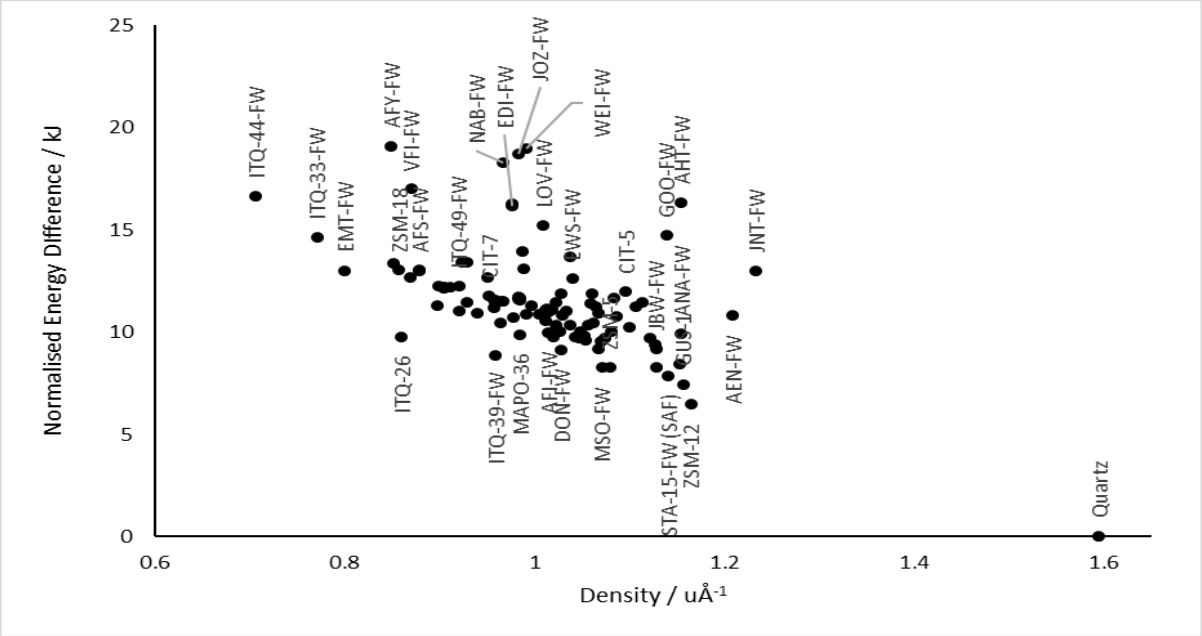

Fig. 3. DFT Normalised Zeolite Energies per T-site with respect to α-Quartz vs Density

More generally, the linear trend highlights the correlation between an increase in cohesive energy and a greater porosity. As noted, this result is in line with expectations as zeolites are known to be metastable with respect to dense structures. The calculated variation of energies against densities is closely related to that obtained with the lattice energy approach with many of the same outlier structures such as NAB, WEI, EDI, LOV and JOZ, suggesting that our previous reasoning regarding outlier structures is sound, as these higher energies transfer across different methodologies and can probably be attributable to the inherent structural characteristics outlined previously. This time ITQ-39 is lower in energy but closer to the general trend than seen with the lattice energy calculations. This result could imply that modelling the electronic contributions with DFT in partially disordered systems can have a significant effect on the overall lattice cohesive energy of a system. ITQ-26 is similarly lower in energy than the general trend but once again the 'real' lattice contains partial occupancies of different elements including Germanium.

3.5 DFT: ALPOs

The same DFT methodology was employed in the optimization of the ALPO structures. The energy difference per T-site was compared to Berlinite and is reported in **Table S5 (see supporting information)**. As can be seen in **Figure**

4, the DFT ALPO study also produced a linear trend like the lattice energy study. There are, however, some nuanced differences such as a large difference in the energies for ALPO-11. In the interatomic potential lattice energy calculations ALPO-11 is close in energy to UiO-6; however, in the DFT study there is a decrease in the energy difference between the two structures from 3.7 kJ to 2.6 kJ. Conversely, ALPO-18 and SAPO-42 are closer in energy to each other than when calculated using DFT (0.6 kJ) than interatomic potentials (2.1 kJ). Overall, the DFT energies are approximately 1 kJ lower in energy than obtained with the lattice energy method.

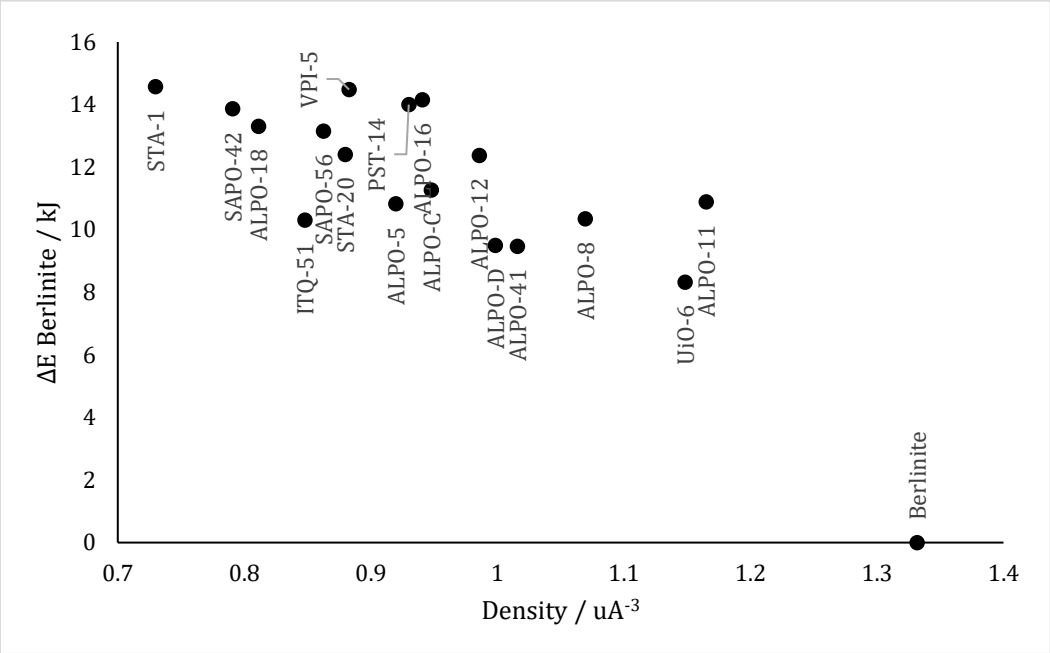

Fig. 4. DFT Normalised ALPO Energies Normalised per T-site with respect to Berlinite vs Density

3.6 Comparison to Experimental Data

When contrasting the energies calculated for zeolites, the interatomic potential, based lattice energy calculations display a linear correlation with the DFT energies, as is shown in **Figure 5**. The ITQ-39 framework is the only noticeable outlier, this discrepancy was highlighted earlier as potentially arising from the disordered nature of the structure.

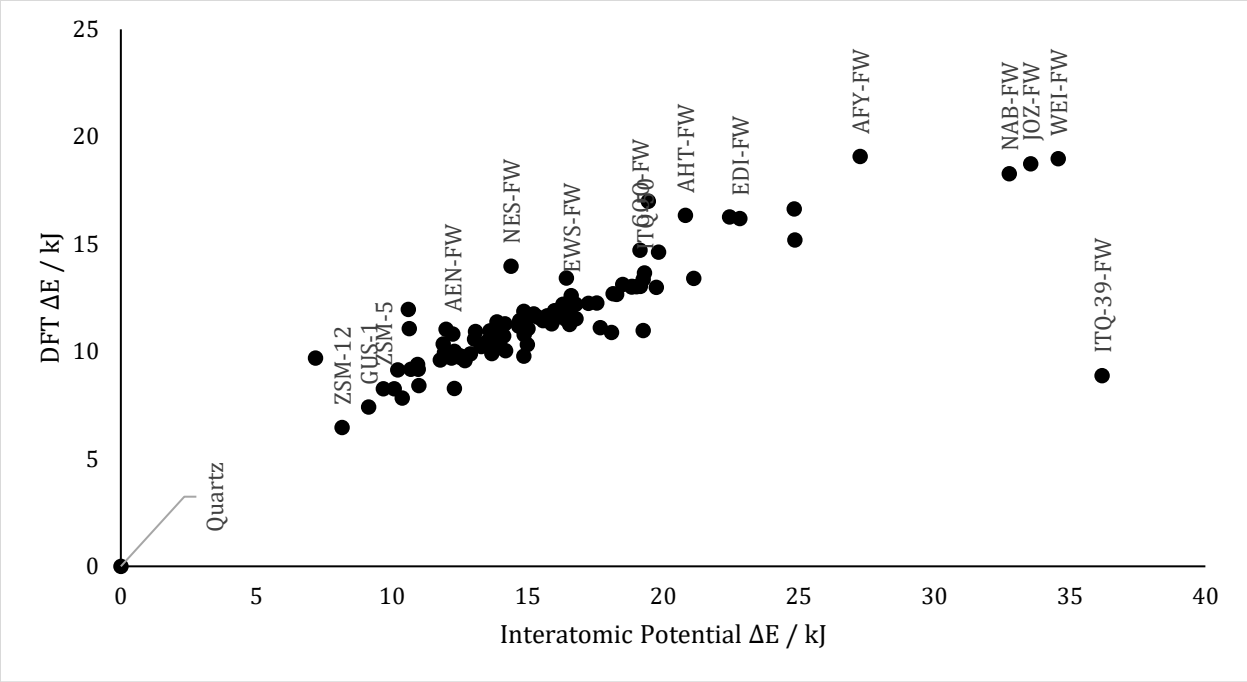

Fig. 5. Correlation between DFT and Interatomic Potential normalized energy differences from α-Quartz

Table 5 compares our calculations with the experimental calorimetric data of Navrotsky and co-workers(Navrotsky et al., 2009; Piccione et al., 2000). We find that the results from lattice energy methodologies are larger than experimental values while the DFT cohesive values are relatively close to the experimental values with generally small discrepancies of 1 – 2 kJ/mol and with only CIT-5 showing an appreciable difference between calculations and experiment.

Structure	I.P. / kJ	DFT / kJ	EXP / kJ	EXP Error / %
AST	18.1	12.7	10.9	± 1.2
BEA	14.4	11.0	9.3	± 0.8
CFI/CIT-5	12.7	12.0	8.8	± 0.8
CHA	16.1	12.2	11.4	± 1.5
IFR/ITQ-4	15.0	10.3	10	± 1.2
ISV/ITQ-7	16.4	13.4	14.4	± 1.1

ITE/ITQ-3	14.1	10.7	10.1	± 1.2
MEL/ZSM-11	10.8	9.2	8.2	± 1.3
MFI/ZSM-5	9.7	8.3	6.8	± 0.8
MWW/ITQ-1	14.4	11.2	10.4	± 1.5
STT/SSZ-23	14.7	11.4	9.2	± 1.2
AFI	11.9	10.0	7.2	NA
EMT	20.1	13.0	10.5	± 0.9
FER	11.8	9.6	6.6	NA
MEI/ZSM-18	18.9	13.0	13.9	± 0.4
MTQ/ZSM-12	8.2	6.5	8.7	NA

Comparison of calculated lattice energies using the Interatomic Potential (I.P.) Shell model (with the Sanders potentials) and DFT compared to experimental values.(Navrotsky et al., 2009; Piccione et al., 2000)

Table 5. Calculated and Experimental Normalised Zeolite Energies per T-site with respect to α-Quartz

We should note that our calculations assume ideal non-defective pure silica frameworks and deviations between calculations and experiment may be attributable to experimental samples having appreciable differences from this ideal state with additional effects and extra-framework species. We also note that we have calculated energies and not enthalpies, but this factor is expected to have a very small effect as our free energy calculations discussed above showed.

Whilst there is less experimental calorimetric data on ALPOs, some are reported by Navrotsky *et al*(Navrotsky et al., 2009) and a different trend is now seen in the comparison between calculations and experiment. This time the interatomic potential method gives values closer to experimental data than the DFT methods as reported in **Table 6**. The poorer agreement between calculations and experiment for the ALPOs may warrant a further in-depth study to determine the reason for such discrepancy. It may relate to the greater differences between the idealised models used in the calculations and the real experimental system; however we note that both sets of calculations were undertaken using the same initial structural data.

Structure	I.P. / kJ	DFT / kJ	EXP / kJ	EXP Error / %
Berlinite	0	0	0	0.54
AST / ALPO-16	12.37	14.15	10.9	10.9
AFI / ALPO-5	6.77	10.83	7.0	2.15
ALPO-8	10.76	10.35	5.56	1.42
ALPO-11	9.10	10.90	6.18	1.17
ALPO-42 (SAPO-42)	12.90	13.87	7.82	1.94
VPI-5	12.60	14.48	8.38	2.26

Experimental values from the work of Navrotsky et al(Navrotsky et al., 2009)

Table 6. Calculated and Experimental Normalised ALPO Energies per T-site with respect to Berlinite

4.0 Summary and Conclusion

For the zeolite structures we have shown that DFT provides more accurate values for the relative energies of microporous structures relative to dense structures than the interatomic potential based methods; indeed most of the DFT energies are within the experimental error of the calorimetric data For the potential based lattice energy calculations, the formal charge shell models are in better agreement with experiment than the partial charge rigid ion model and can provide a good reproduction of trends observed in both DFT and experiment at a low computational cost. However, the interatomic potential method has a propensity to over-estimate lattice energies by a significant margin. In zeolites this discrepancy may be due to the inability of the potential based approach to model charge redistribution on transforming from dense to microporous metastable phases, which can, of course, be modelled in DFT studies.

The opposite result was observed in the modelling of the ALPO systems. Interatomic potential calculations yielded more accurate energies than the DFT methodology when compared to experimental values. This result may be attributable to the stronger deviation of real experimental ALPOs from the ideal assumed by our calculations. Overall, our results suggest that the DFT methodologies used here can provide a quantitative estimate of the energetics of microporous relative to dense frameworks, while the computationally cheaper potential-based methods provide a good guide to overall trends.

5.0 ACKNOWLEDGMENTS

We are grateful to Professor Avelino Corma for many stimulating discussions concerning zeolite structures stabilites and reactivities over many years.Computing facilities for this work were provided by ARCCA at Cardiff University, HPC Wales, and through our membership of the U.K.'s Materials Chemistry Consortium (MCC). Catalysis Hub Consortium is funded by EPSRC (grants EP/ R026815/1, EP/K014854/1, and EP/M013219/1). The MCC is funded by EPSRC (EP/F067496).

6.0 REFERENCES

Buckingham, R. A., Buckingham, & A., R. (1938). The Classical Equation of State of Gaseous Helium, Neon and Argon. *RSPSA*, *168*(933), 264–283. https://doi.org/10.1098/RSPA.1938.0173

Ch. Baerlocher and L.B. McCusker. (n.d.). *Database of Zeolite Structures*. Http://Www.Iza-Structure.Org/Databases/. Retrieved 21 May 2020, from http://www.iza-structure.org/databases/

Cope, E. R., & Dove, M. T. (2007). Pair distribution functions calculated from interatomic potential models using the General Utility Lattice Program. *Journal of Applied Crystallography*, *40*(3), 589–594. https://doi.org/10.1107/S0021889807016032

Cundy, C. S., & Cox, P. A. (2003). The hydrothermal synthesis of zeolites: History and development from the earliest days to the present time. *Chemical Reviews*, *103*(3), 663–701. https://doi.org/10.1021/CR020060I/ASSET/IMAGES/LARGE/CR020060IF00021.JPEG

Dick, B. G., & Overhauser, A. W. (1958). Theory of the Dielectric Constants of Alkali Halide Crystals. *Physical Review*, *112*(1), 90–103. https://doi.org/10.1103/PhysRev.112.90

Dorta-Urra, A., & Gulín-González, J. (2006). A computational investigation on substitution of magnesium for aluminium in AlPO4-5 microporous material. *Microporous and Mesoporous Materials*, *92*(1–3), 109–116. https://doi.org/10.1016/j.micromeso.2005.12.009

Fischer, M., & Angel, R. J. (2017). Accurate structures and energetics of neutral-framework zeotypes from dispersion-corrected DFT calculations. *The Journal of Chemical Physics*, *146*(17), 174111. https://doi.org/10.1063/1.4981528

Fischer, M., Evers, F. O., Formalik, F., & Olejniczak, A. (2014). Benchmarking DFT-GGA calculations for the structure optimisation of neutral-framework zeotypes. *Theor Chem Acc*, *135*, 257. https://doi.org/10.1007/s00214-016-2014-6

Gale, J. D. (1997). GULP: A computer program for the symmetry-adapted simulation of solids. *Journal of the Chemical Society, Faraday Transactions*, *93*(4), 629–637. https://doi.org/10.1039/A606455H

Gale, J. D. (2005). GULP: Capabilities and prospects. *Zeitschrift Fur Kristallographie*, *220*(5–6), 552–554. https://doi.org/10.1524/ZKRI.220.5.552.65070/MACHINEREADABLECITATION/RIS

Gale, J. D. (2006). Empirical potential derivation for ionic materials. *Https://Doi.Org/10.1080/13642819608239107*, *73*(1), 3–19. https://doi.org/10.1080/13642819608239107

Gale, J. D., & Henson, N. J. (1994). Derivation of Interatomic Potentials for Microporous Aluminophosphates from the Structure and Properties of Berlinite. *J. CHEM. SOC. FARADAY TRANS*, *20*, 3175–3179.

Gale, J. D., Raiteri, P., & van Duin, A. C. T. (2011). A reactive force field for aqueous-calcium carbonate systems. *Physical Chemistry Chemical Physics*, *13*(37), 16666–16679. https://doi.org/10.1039/C1CP21034C

Gale, J. D., & Rohl, A. L. (2010). An efficient technique for the prediction of solvent-dependent morphology: the COSMIC method. *Http://Dx.Doi.Org/10.1080/08927020701713902*, *33*(15), 1237–1246. https://doi.org/10.1080/08927020701713902

Gale, J. D., & Rohl, A. L. (2011). The General Utility Lattice Program (GULP). *Http://Dx.Doi.Org/10.1080/0892702031000104887*, *29*(5), 291–341. https://doi.org/10.1080/0892702031000104887

González, J. G., Alcaz, J. D. L. C., Ruiz-Salvador, A. R., Gómez, A., Dago, A., & de Las Pozas, C. (1999). Computational study of substitution of Al by Fe3+ in the AlPO4-5 framework. *Microporous and Mesoporous Materials*, *29*(3), 361–367. https://doi.org/10.1016/S1387-1811(99)00005-0

Grimme, S., Antony, J., Ehrlich, S., & Krieg, H. (2010). A consistent and accurate ab initio parametrization of density functional dispersion correction (DFT-D) for the 94 elements H-Pu. *The Journal of Chemical Physics*, *132*(15), 154104. https://doi.org/10.1063/1.3382344

Henson, N. J., Cheetham, A. K., & Gale, J. D. (1994). Theoretical Calculations on Silica Frameworks and Their Correlation with Experiment. In *Chemistry of Materials* (Vol. 6, Issue 10). https://doi.org/10.1021/cm00046a015

Henson, N. J., Cheetham, A. K., & Gale, J. D. (1996). Computational studies of aluminum phosphate polymorphs. *Chemistry of Materials*, *8*(3), 664–670. https://doi.org/10.1021/CM9503238

Joubert, D., Kresse, G., & Joubert, D. (1999). From Ultrasoft Pseudopotentials to the Projector Augmented-Wave Method One dimensional Lattice Density Functional Theory View project First-Principles Calculations of the Electronic and Optical Properties of CH 3 NH 3 PbI 3 for Photovoltaic Applications View project From ultrasoft pseudopotentials to the projector augmented-wave method. *Article in Physical Review B*. https://doi.org/10.1103/PhysRevB.59.1758

Kresse, G., & Furthmüller, J. (1996a). Efficiency of ab-initio total energy calculations for metals and semiconductors using a plane-wave basis set. *Computational Materials Science*, *6*(1), 15–50. https://doi.org/10.1016/0927-0256(96)00008-0

Kresse, G., & Furthmüller, J. (1996b). Efficient iterative schemes for ab initio total-energy calculations using a plane-wave basis set. *Physical Review B*, *54*(16), 11169. https://doi.org/10.1103/PhysRevB.54.11169

Kresse, G., & Hafner, J. (1993). Ab initio molecular dynamics for liquid metals. *Physical Review B*, *47*(1), 558. https://doi.org/10.1103/PhysRevB.47.558

Kresse, G., & Hafner, J. (1994). Ab initio molecular-dynamics simulation of the liquid-metal–amorphous-semiconductor transition in germanium. *Physical Review B*, *49*(20), 14251. https://doi.org/10.1103/PhysRevB.49.14251

Majda, D., Almeida Paz, F. A., Delgado Friedrichs, O., Foster, M. D., Simperler, A., Bell, R. G., & Klinowski, J. (2008). *Hypothetical Zeolitic Frameworks: In Search of Potential Heterogeneous Catalysts*. https://doi.org/10.1021/jp0760354

Navrotsky, A., Trofyrnluk, O., & Levchenko, A. A. (2009). Thermochemistry of microporous and mesoporous materials. *Chemical Reviews*, *109*(9), 3885–3902. https://doi.org/10.1021/cr800495t

Ogata, K., Takeuchi, Y., & Kudoh, Y. (1987). Structure of α-quartz as a function of temperature and pressure. *Zeitschrift Für Kristallographie - Crystalline Materials*, *179*(1–4), 403–414. https://doi.org/10.1524/ZKRI.1987.179.14.403

Perdew, J. P., Burke, K., & Ernzerhof, M. (1996). Generalized Gradient Approximation Made Simple. *Physical Review Letters*, *77*(18), 3865. https://doi.org/10.1103/PhysRevLett.77.3865

Perdew, J. P., & Zunger, A. (1981). Self-interaction correction to density-functional approximations for many-electron systems. *Physical Review B*, *23*(10), 5048. https://doi.org/10.1103/PhysRevB.23.5048

Piccione, P. M., Laberty, C., Yang, S., Camblor, M. A., Navrotsky, A., & Davis, M. E. (2000). Thermochemistry of pure-silica zeolites. *Journal of Physical Chemistry B*, *104*(43), 10001–10011. https://doi.org/10.1021/jp002148a

Pophale, R., Cheeseman, P. A., & Deem, M. W. (2011). A database of new zeolite -like materials. *Physical Chemistry Chemical Physics*, *13*(27), 12407–12412. https://doi.org/10.1039/C0CP02255A

Román-Román, E. I., & Zicovich-Wilson, C. M. (2015). The role of long-range van der Waals forces in the relative stability of SiO2-zeolites. *Chemical Physics Letters*, *619*, 109–114. https://doi.org/10.1016/J.CPLETT.2014.11.044

Sanders, M. J., Leslie, M., & Catlow, C. R. A. (1984). Interatomic potentials for SiO2. In *Journal of the Chemical Society, Chemical Communications* (Issue 19). https://doi.org/10.1039/c39840001271

Sowa, H., Macavei, J., & Schultz, H. (1990). The crystal structure of berlinite AlPO4 at high pressure. *Zeitschrift Für Kristallographie - Crystalline Materials*, *192*(1–4), 119–136. https://doi.org/10.1524/ZKRI.1990.192.14.119

Stojakovic, D., & Rajic, N. (2001). Computational studies in the AlPO4-34 system. In *Journal of Porous Materials* (Vol. 8, Issue 3). https://doi.org/10.1023/A:1012296908560

van Beest, B. W. H., Kramer, G. J., & van Santen, R. A. (1990). Force fields for silicas and aluminophosphates based on ab initio calculations. *Physical Review Letters*, *64*(16), 1955–1958. https://doi.org/10.1103/PhysRevLett.64.1955